Title

Combined use of statistical and DInSAR data analyses to define the state of activity of slow-moving landslides

Authors

Calvello Michele[1*], Peduto Dario[2], Arena Livia[3]

[1*] Corresponding Author, University of Salerno, Dep. Civil Engineering, Via Giovanni Paolo II 132, 84084 Fisciano SA, Italy, michele.calvello@gmail.com, +39 349 6830767

[2] University of Salerno, Dep. Civil Engineering, Via Giovanni Paolo II 132, 84084 Fisciano SA, Italy, dpeduto@unisa.it

[3] University of Salerno, Dep. Civil Engineering, Via Giovanni Paolo II 132, 84084 Fisciano SA, Italy, liviaarena@libero.it

Keywords

Slow-moving landslides; statistical analyses; DInSAR; zoning

Abstract

Statistical analyses have been often used for landslide susceptibility zoning at small to medium scale when relevant base and thematic maps are available. Since the beginning of the last decade, images remotely acquired by spaceborne Synthetic Aperture Radar (SAR) and processed via Differential SAR Interferometry (DInSAR) proved extremely useful for non-invasive and non-destructive monitoring of displacements of the topographic surface. The present paper proposes an original procedure for the definition of the state of activity of slow-moving landslides via the combined use of multivariate statistical analyses and DInSAR data. The procedure is based on the following essential elements: distinction between terrain units used for computational purposes and the final zoning units; independent statistical and DInSAR analyses and activity models leading to first level state of activity zoning maps; a consistency model between statistical and DInSAR analyses; two confidence and combination models leading, respectively, to second or third level state of activity zoning maps. The application in a test area including 19 municipalities in southern Italy, where slow-moving landslides are widespread and accurately mapped by using geomorphological criteria, allowed the generation of the three above-mentioned levels of zoning maps. The results were successfully crosschecked by exploiting a different DInSAR dataset and the results of previous works based on the use of slow-moving landslide-induced damage to facilities surveys.

1. Introduction

Slow-moving active landslides are phenomena, widespread all over the world, which do not pose major risks to human lives but systematically cause significant damage to structures and infrastructures (D'Elia and Rossi-Doria, 2000; Picarelli and Russo, 2004; Spizzichino et al., 2004; Bonnard et al., 2008; Wang et al., 2008; Urciuoli and Picarelli, 2008; Mansour et al., 2011; Ferlisi et al., 2015; Peduto et al., 2016). To cope with the costs associated to the damage caused over large portions of the territory by slow-moving active landslides, such as deep-seated rotational and translational slides and earth flows (Varnes, 1978; Cruden and Varnes, 1996), effective risk management strategies are needed. The first step of landslide risk management is, according to the framework proposed by Fell et al. (2005), hazard analysis, which involves characterizing the landslide and the corresponding frequency of occurrence, i.e. "a measure of likelihood expressed as the number of occurrences of an event in a given time or in a given number of trials". When the event is a slow-moving landslide, frequency analysis must be based on the analysis and forecast of the kinematic behavior of the phenomenon. In other words, the analysis of the frequency of slow-moving landslides turns into the evaluation of their past, current and future state of activity. Over large portions of the territory, this evaluation needs the application of strategies and models leading to susceptibility zoning—a quantitative or qualitative assessment of the classification, volume and spatial distribution of landslides which exist or potentially may occur in an area (Fell et al., 2008)—and hazard zoning—which takes the outcomes of landslide susceptibility mapping and assigns an estimated frequency to the potential landslides (Fell et al., 2008).

Numerous studies evaluated landslide susceptibility over large portions of the territory by means of data driven statistical analyses (e.g., Carrara, 1983; Guzzetti et al., 1999; van Westen, 2004). Typically, susceptibility zoning maps are generated by a model relating

known landslide occurrences to relevant thematic layers by exploiting the principle that "the past and present are keys to the future" (Varnes, 1984). Yet, if the aim of the susceptibility analysis is the possible reactivation of existing slow-moving landslides, a reliable susceptibility model must consider, in addition to the presence of past landslides in the territory to be zoned, some objective information regarding the past and current state of activity for the phenomena (Calvello et al., 2013). A valuable contribution on the evaluation of the hazard posed by slow-moving landslides over large portions of the territory is offered by remote sensing techniques, which are able to retrieve ground displacement information by either passive or active air- and space-borne sensors. Among these, particularly effective have proved to be algorithms developed to deal with Synthetic Aperture Radar Differential Interferometry data (e.g., Ferretti et al., 2000; Berardino et al., 2002) in studies concerning slow-moving landslides in different geological contexts all over the world (e.g., Catani et al., 2005; Tofani et al., 2013; Cascini et al., 2013a; Antronico et al., 2013; Lu et al., 2014; Wasowski and Bovenga, 2014; Gullà et al. 2016).

In this paper, a procedure is proposed to define the state of activity of slow-moving landslides over large portions of the territory by combining the results of statistical multivariate analyses and DInSAR data analyses. The products of the analyses are state of activity zoning maps which classify in four classes—descriptors: Very Low, Low, Medium and High—existing landforms susceptible to slow landsliding herein called, following Calvello et al. (2013), Terrain Zoning Units. The state of activity zoning maps are differentiated in three levels depending on the way they employ the results of the two analyses. The effectiveness of the adopted procedure is tested for a study area in Southern Italy where widespread slow-moving landslides have been accurately mapped using geomorphological criteria.

2. Statistical and DInSAR analyses for landslide studies

2.1. Statistical methods for landslide zoning at medium scale

Data driven methods using statistical techniques for assessing landslide susceptibility and hazard over large areas, typically at scales ranging 1:10.000 to 1:100.000, have long been performed and described within the international literature (Carrara 1983; Guzzetti et al., 1999; Dai and Lee, 2002; Chung and Fabbri, 2003; van Westen, 2004; Thiery et al., 2007; Pourghasemi et al., 2012; Calvello et al., 2013; Taskin et al., 2015; Ciurleo et al. 2016; among others). Statistical methods may be classified in two main categories, according to whether they employ bivariate and multivariate techniques (Figure 1). Both types of analysis rely on the information provided by: a landslide event map derived from a landslide inventory, which acts in the analyses as the only dependent variable; a number of thematic independent variables pre-identified as possible causal factors for landslide events. Weights are computed and assigned to the independent variables considering their statistical importance, both in absolute and relative terms, for detecting landslide events in the study area. Examples of bivariate statistical models used in landslide susceptibility and hazard studies are: likelihood ratios (Chung, 2006; Lee et al., 2007; Dewitte et al., 2010); weights of evidence (Mathew et al., 2007; Pradhan et al., 2010); information value (Yin and Yan, 1988). Examples of multivariate statistical models are: discriminant analysis (Baeza and Corominas, 2001; Rossi et al., 2010); logistic regression (Chau and Chan, 2005; Van Den Eeckhaut et al., 2006; Bai et al., 2010); artificial neural networks (Ermini et al., 2005; Nefeslioglu et al., 2008).

In the majority of these studies, landslide susceptibility and hazard zoning maps are generated by models relating known landslide occurrences to relevant thematic layers. This is often an appropriate assumption, such as when the analysis deals with the first failures of fast-moving phenomena and employs landslide event maps created using well-defined triggering factors,

yet this is not always true. For instance, if the aim of a susceptibility analysis is the possible reactivation of existing slow-moving landslides, a reliable susceptibility model must consider, in addition to the presence of past landslides in the territory to be zoned, some objective information regarding the past and current state of activity for the phenomena. In such cases, a statistical correlation between existing landslides and relevant geomorphological predisposing factors may still be valuable if it used as part of a procedure employing such information. This is, indeed, the approach used within the procedure presented hereafter, wherein the information on the state of activity of existing slow-moving landslides is retrieved from an analysis of available DInSAR data. It worth highlighting that the proposed procedure does not endorse any specific statistical methodology, but rather prescribes the relationships needed to move from zoning maps derived from statistical or DInSAR data analysis (Peduto et al., 2015a) to zoning maps taking advantage of the combined use of both sources of information.

2.2. Multipass DInSAR techniques and their applications for landslide characterization

Multi-pass DInSAR algorithms have been successfully used to derive information on displacements of the topographic surface since early 2000s (Peduto et al., 2015b). The analysis of phase signals in interferometric stacks can be carried out via different techniques grouped in two main classes : Persistent Scatterers Interferometry, PSI (Ferretti et al., 2000, 2001; Costantini et al., 2008; Crosetto et al., 2008), and Small Baseline, SBAS, approaches (Berardino et al., 2002; Fornaro et al., 2009). An upgrade of the PSI techniques (SQUEESAR, Fumagalli et al., 2011) has been developed for monitoring distributed scatterers by using multilooking during the data processing.

The DInSAR dataset available for the analyses carried out in the present paper results from the application of a PSI technique (Ferretti et al., 2001; Costantini et al., 2008). Persistent Scatterers (PS) can be identified as a subset of coherent radar targets usually corresponding to man-made structures (e.g., buildings, roads) or natural targets (e.g., bare rocks) on the ground. PS-derived velocity are acquired along the radar Line Of Sight (LOS) with reference to a fixed point on the ground (reference point) and with a sub-millimetre accuracy or the average velocity and sub-centimetre accuracy on the single displacement measure. Each PS is associated with a coherence value (ranging from 0 up to 1) which indicates how the measure fits the model assumed for the displacement.

At present the scientific literature counts a number of papers focusing on the application of PSI—and more generally DInSAR—techniques to analyze displacements associated with slow-moving landslides (Colesanti and Wasowski, 2006; Cascini et al., 2009, 2010; Wei and Sandwell, 2010; Bianchini et al., 2014; Wasowski and Bovenga, 2014). The use of DInSAR data for slow-moving landslide characterization and mapping has been investigated at different scales of analysis (Fell et al., 2008): small, i.e. <1:100.000 (Meisina et al., 2008); medium, i.e. from 1:100.000 to 1:25.000 (Catani et al., 2005; Cascini et al., 2009, 2010; Lu et al., 2014; Zhang et al., 2014); large, i.e. from 1:25.000 to 1:5000 (Notti et al., 2010); detailed, i.e. >1:5000 (Colesanti et al., 2003; Herrera et al., 2011; Calò et al. 2014; Gullà et al., 2016). The types of slow-moving landslides investigated in the aforementioned studies are mainly (Tofani et al., 2013): slides and earth flows, deep-seated gravitational movements and creep phenomena.

The PSI data used in the present study were collected within the Piano Straordinario di Telerilevamento-PST (MATTM, 2010), which is a project supported by the Italian Ministry of Environment, Land and Sea covering all the Italian territory with an ERS-ENVISAT sensor

database of almost 20 years since 1992. The following data are available for the study area: 208 ERS images on ascending orbit (from September 1992 to September 2000); 134 ERS on descending orbit (from November 1992 to December 2000); 52 ENVISAT images on ascending orbit (from November 2002 to July 2010); 49 ENVISAT on descending orbit (from March 2003 to June 2010). In the next sections the possibility of integrating, for landslide zoning purposes, DInSAR data with the results of multivariate statistical analysis is shown.

3. Procedure to define the state of activity of slow-moving landslides at regional scale

A procedure is herein proposed to define the state of activity of slow-moving landslides at regional scale on the basis of: an inventory of existing landforms susceptible to slow landsliding; statistical multivariate and DInSAR data analyses carried out, over the study area, using available thematic information. The products of the analyses are "state of activity zoning maps" (Figure 2), which can be distinguished in: first level zoning maps, if achieved by single information analyses (either DInSAR or statistical); second level zoning maps, if an additional value, in terms of reliability, is provided by the complementary information derived from the analysis of the companion dataset; third level zoning maps, if the outcomes of the DInSAR and statistical analyses are fully merged.

The procedure is based on the following essential elements:

- distinction between Terrain Computational Units, TCU, which refer to territorial domains used to define, calibrate and/or validate a model for landslide analyses, and Terrain Zoning Units, TZU, which are units used to produce a landslide map for zoning purposes (Calvello et al. 2013);
- independent statistical/DInSAR analyses and activity models, respectively leading to first level computational and zoning maps;

- a consistency model between statistical and DInSAR analyses based on the comparison between the two first level computational maps;
- statistical/DInSAR confidence models, based on the first level zoning maps and on appropriately defined combination statistics from the consistency model, leading to second level state of activity zoning maps;
- two combination models, respectively leading to second or third level state of activity zoning maps according to whether or not they employ the information provided by the confidence models.

First level zoning maps

The statistical analysis leading to first level computational and zoning maps should be performed in two steps. The first step of the analysis leads to a dichotomous statistical computational map, wherein TCU are distinguished as “active” or “not active”. Such analysis is based on the information provided by an event map, derived from a landslide inventory wherein the state of activity of slow-moving landslides is explicitly defined, and a series of relevant independent variables derived from available thematic maps. To this purpose, any multivariate statistical methodology able to weight independent variables based on the information provided by a dependent variable is appropriate (Baeza and Corominas 2001; Guzzetti et al. 2005; Chau and Chan 2005, among many others). Within this phase the independent variables are derived from the thematic maps based on numerical algorithms that consider the characteristics of the statistical model and the features of the input data. For instance, qualitative thematic variables may need to be transformed into quantitative variables or dimensionless variables may be necessary. The event map is always defined as the subset of slow-moving landslides classified as active according to a landslide inventory, typically following geomorphological criteria. The second step of the statistical analysis leads to a state of activity zoning map based on an activity model. The statistical activity model (Figure 3a)

relies on the computation, over each TZU, of a statistical Index of Activity (IA_S) defined as the ratio between the number of active TCUs (TCU_a) and the total number of TCUs (TCU_{tot}):

$$IA_S = \frac{TCU_a}{TCU_{tot}} \quad \text{(Eq.1)}$$

The statistical state of activity zoning map is drawn associating to each TZU one of four possible activity indicators, considering the computed IA_S values as follows: high activity ($0.7 \leq IA_S \leq 1$); medium activity ($0.35 \leq IA_S < 0.7$); low activity ($0.05 \leq IA_S < 0.35$); very low activity ($0 \leq IA_S < 0.05$).

Concerning the analysis of DInSAR data (Peduto et al., 2015a), the first step deals with the identification of the monitoring data available for each TCU and with the definition of a movement threshold value. TCUs are classified as “covered” or “not covered” by DInSAR data, depending on the availability of DInSAR information within their perimeter. An average velocity value is then computed for each TCU covered by DInSAR data following the procedure described by Cascini et al. (2013a, 2013b), which operates considering the coherence values associated with DInSAR data as quality weights. A covered TCU is defined as “moving” or “not moving” according to whether or not the computed weighted velocity exceeds a specified threshold value. The results of this step of the analysis is a DInSAR computational map wherein the grid cells assume one of three possible values: not covered, covered and moving; covered and not moving. In the second step of the DInSAR analysis, the TZUs are used to produce, via the definition of an activity model, a DInSAR state of activity zoning map. The DInSAR activity model (Figure 3b) is based on the computation, over each TZU, of a DInSAR Index of Activity (IA_D), as in Peduto et al. (2015a). The latter is defined

as the ratio, within the TZU, between the number of covered and moving TCUs (TCU_{cm}) and the number of covered TCUs (TCU_c):

$$IA_D = \frac{TCU_{cm}}{TCU_c} \quad \text{(Eq.2)}$$

The final map of the DInSAR analysis, i.e. the state of activity zoning map, is drawn associating to each TZU one of four possible activity indicators, defined considering the computed IA_D values as follows: high activity ($0.7 \leq IA_D \leq 1$); medium activity ($0.35 \leq IA_D < 0.7$); low activity ($0.05 \leq IA_D < 0.35$); very low activity ($0 \leq IA_D < 0.05$).

Second level zoning maps

As shown in Figure 2, a first step toward the joint use of the statistical and DInSAR analyses within this phase of the procedure is represented by the definition of a consistency model, which aims at crosschecking the information provided, over each TCU, by the two analyses. The consistency model proposed herein may be represented by a 2 by 2 matrix (Figure 4a), whose elements are defined as the number of TCUs: moving according to the DInSAR analysis and active according to the statistical analysis ($TCU_{M/A}$); not-moving according to the DInSAR analysis and active according to the statistical analysis ($TCU_{NM/A}$); moving according to the DInSAR analysis and not-active according to the statistical analysis ($TCU_{M/NA}$); not-moving according to the DInSAR analysis and not-active according to the statistical analysis ($TCU_{NM/NA}$). Combinations “M/A” and “NM/NA” indicate consistency between the information provided by the two analyses, while the other two combinations indicate a lack of consistency between DInSAR data and the results of the statistical analysis. The total number of TCUs considered in the matrix is equal to the number of TCUs covered by DInSAR data (TCU_c).

The two confidence models needed to get to the second level zoning maps are defined on the basis of statistics derived from the consistency matrix. In particular, the following formulas are used to compute, over each TZU, a true-positives consistency index, $IC_{M/A}$, and a true-negatives consistency index, $IC_{NM/NA}$, respectively defined as follows:

$$IC_{M/A} = \frac{TCU_{M/A}}{TCU_c} \quad \text{(Eq.3)}$$

$$IC_{NM/NA} = \frac{TCU_{NM/NA}}{TCU_c} \quad \text{(Eq.4)}$$

The consistency indexes are used both for the statistical and the DInSAR confidence models (Figures 4b and 4c). The models simply add, for each TZU, a confidence attribute to the activity indicators defined in the first level state of activity zoning map. Two confidence attributes are used: “high confidence” (hc), for consistency index values higher than 0.5; “low confidence” (lc), for consistency index values lower or equal to 0.5. In particular, if the activity indicator is either High or Medium, Eq. 3 ($IC_{M/A}$) is used to assign the confidence attributes. Whereas, if the activity indicator is either Low or Very Low, Eq. 4 ($IC_{NM/NA}$) is used to assign the confidence attributes. The two resulting zoning maps are called, respectively: statistical state of activity zoning map with confidence level; DInSAR state of activity zoning map with confidence level (Peduto et al., 2015a). Each map employs the following eight zoning classes: high activity, computed with a high confidence level (H_{hc}); high activity, computed with a low confidence level (H_{lc}); medium activity, computed with a high confidence level (M_{hc}); medium activity, computed with a low confidence level (M_{lc}); low activity, computed with a high confidence level (L_{hc}); low activity, computed with a low

confidence level (L_{lc}); very low activity, computed with a high confidence level (VL_{hc}); very low activity, computed with a low confidence level (VL_{lc}).

At this level of analysis, an alternative combination of the two first level zoning maps could be performed by fully merging the two maps without using a confidence model. To this aim, a combination model needs to be defined (Figure 4d). The combination model used herein is symmetric, thus the information derived from the two analyses is weighted equally. The state of activity indicators used to classify the TZUs are five. Indeed, besides the four activity indicators already used within the first level zoning maps (high, medium, low and very low), another indicator is needed to identify the TZUs for which the results of the two analysis are very different from one another. The resulting map, which is called combined statistical-DInSAR state of activity zoning map, is drawn associating to each TZU one of the following five activity indicators: high activity (H), if the highest value of at least one activity indicator is high and the lowest value is, at most, medium; medium activity (M), if the highest value of at least one activity indicator is medium and the lowest value is never very low; low activity (L), if the highest value of at least one of the two activity indicators is low; very low activity (VL), if both activity indicators are very low; further scrutiny needed (S), if the two activity indicators differ by more than two levels.

Third level zoning map

The final product of the procedure is a map, which is called high confidence statistical-DInSAR state of activity zoning map, derived by fully merging the results of the two analyses. To this aim, the combined statistical-DInSAR state of activity zoning map is filtered to consider only the Terrain Zoning Units characterized by a high confidence level (hc). The combination model used to derive the final zoning map is shown in Figure 5. Evidently, the

resulting zoning map only classifies a reduced number of the TZU available in the two first level zoning maps. Yet, this subset of classified landforms may be considered of special value because the reported state of activity is based on evaluations showing a high level of consistency between the two employed methodologies.

4. A case study in southern Italy

The proposed procedure has been applied and tested in a study area of about 490 km^2 (Figure 6) including 19 municipalities of the Campania region in southern Italy, within the territory of the National Basin Authority of the Liri-Garigliano and Volturno rivers. The area was selected for two main reasons: the widespread presence of slow-moving landslides, covering about 21% of the territory; the availability of previous studies combining DInSAR data and damage survey analysis to evaluate the state of activity of slow-moving landslides (Cascini et al., 2013a).

The available dataset consists of topographic maps and thematic maps at 1:25,000 scale. These maps were developed during the activities carried out by the National Basin Authority within the hydrogeological regional planning for landslide risk following the Italian Law 365/2000. The geological map of the area highlights the existence of Mesozoic–Tertiary lithological units mainly consisting of clayey-sandy-arenaceous and clayey calcareous-siliceous strata covered by mTCUcmarly-calcareous, arenaceous and arenaceous-conglomeratic units (Rapolla et al., 2012; Cascini et al., 2013a). These latter units together with the geostructural setting mainly control the geomorphological features of the area.

The available landslide inventory map (Figure 6)—developed on the basis of geomorphological criteria supported by field surveys and aerial photo interpretation—provides detailed information for each mapped phenomenon with reference to location, type,

state of activity and areal extension. As far as the type of phenomenon is concerned, over a total number of 1897 reported slow-moving landslides, the inventory map distinguishes: 1001 earth flows; 671 rotational slides; 225 composite rotational slides/earth flows. These landslides are further classified according to two possible states of activity, "dormant" and "active", the latter including active, reactivated and suspended phenomena (Cruden and Varnes, 1996). The size of the mapped landslides ranges from about 1000 m^2 to about 2,000,000 m^2, with an average value of 54,000 m^2. It is worth pointing out that dormant phenomena, which amount 1372, clearly prevail in number over active ones.

4.1. Application of the proposed procedure

As stated in the previous section, the proposed procedure is based on the distinction between terrain computational units related to the spatial resolution of the map, TCUs, and terrain zoning units related to the desired informative resolution of the zoning, TZUs. The analyses conducted herein employ: the digital elevation model built on a 25m by 25 m square grid to define the TCUs; the landslide inventory map to identify the TZUs, i.e. the landforms susceptible to slow landsliding wherein the state of activity zoning is to be determined. The TZUs employed in the analyses are the slow-moving landslides classified as dormant, according to geomorphological criteria, within the employed landslide inventory. Following these choices, the total number of TCUs and TZUs within the study area amount, respectively, to 835,335 and 1372.

First level analyses and maps

The input data for the statistical analysis comprise seven independent variables derived from available thematic maps (Figure 7) and one dependent variable, called the event map, which

derives from the available landslide inventory map. Concerning the dependent variables, one of them (geo-litological units) is a categorical variable with 11 different classes; the rest are numeric variables, three of them (elevation, slope, curvature) derived from the available digital elevation model and three of them (distance from river network, distance from faults and distance from springs) derived from categorical vector maps. All the numeric variables have been classified using a quantile criterion with eight classes, i.e. each class includes about 12.5% of the total population (Table 1).

The statistical procedure employed herein is known in the literature with the name of "information value method" (e.g. Yin and Yan, 1988) and is based on many bivariate analyses between each independent variable and a dichotomous dependent variable, i.e. the event map. The multivariate statistical analysis was carried out assuming as event map the sample of the active slow-moving landslides mapped in the inventory map. Following the procedure described in Figure 2, the first purpose of the statistical analysis was to produce a computational map, covering the whole study area, wherein active TCUs (herein called TCU_a) are determined on the basis of a functional multivariate relationship between the dependent and the independent variables. In this case, the relevant dependent variable employed to produce the final computational are three: geo-litological units, elevation and slope. The second step of the statistical analysis is based on an activity model and leads, as for the DInSAR analysis, to a state of activity zoning map. The statistical activity model relies on the computation, over each TZU, of a statistical Index of Activity, IA_S (Eq. 1), defined as the ratio between the number of active computational units, TCU_a, and the total number of computational units, TCU_{tot}. As already mentioned, the activity indicators are the following four: high activity; medium activity; low activity; very low activity. Figure 8 shows the computation and state of activity zoning maps resulting from the statistical analysis and from

the related activity model. Already by looking at the computational map (Figure 8a), it emerges that most the TZUs are not covered by a significant number of active TCUs. Consistently, the state of activity zoning map (Figure 8b) classifies over 57% of the 1372 TZUs as low activity or very low activity units.

The dataset used for the DInSAR analysis is shown in Figure 9 with reference to ERS and ENVISAT data. ERS data exhibit a density of 45.6 PS/km^2; this value increases up to 96.0 PS/km^2 for ENVISAT data. Figure 10 shows the computation and state of activity zoning maps resulting from the DInSAR analysis, carried out employing ERS data, and from the related activity model. ERS data were chosen over ENVISAT data for the analyses carried out herein because they refer to a period (from 1992 to 2000) which can be related to the employed landslide inventory map developed, at the beginning of the 2000's, according to geomorphological criteria. The DInSAR computational map (Figure 10a) was derived by setting a movement threshold of 1.5 mm/year (Cascini et al., 2009, 2010) on the L.O.S. average velocity values (Cascini et al., 2013a) computed for each TCU. In such a way, 14.472 TCUs were identified as "covered", 2% of them classified as moving and 98% of them as not moving. Then, the computation of the DInSAR Index of Activity, IAD (Eq. 2), allowed the application of the DInSAR activity model. The resulting state of activity zoning map (Figure 10b) is drawn, as already described in the previous section, associating to each TZU one of four possible activity indicators: high activity; medium activity; low activity; very low activity. The state of activity map reports, over the considered sample of 272 DInSAR covered terrain units, the following distribution: 72 high activity TZUs; 25 medium activity TZUs; 35 low activity TZUs; 140 very low activity TZUs.

A synthesis of the zoning maps resulting from the two analyses is presented in Table 2, which reports the classification of relevant TZUs in the following three cases: i) statistical state of

activity zoning map, considering the sample of 1372 TZUs characterized by the statistical analysis; ii) statistical state of activity zoning map, considering the sample of 272 TZUs characterized by both the statistical and the DInSAR analyses; iii) DInSAR state of activity zoning map, considering the sample of 272 TZUs characterized by the DInSAR analyses. As the latter two cases refer to the same sample of TZUs, the results may be directly compared. They do not reveal significant differences between the two analyses, yet the state of activity distribution from the DInSAR analyses of the TZU analysis is slightly more polarized towards the two extreme classes.

Second and third level maps

The results of the first level analyses have been combined, following the procedure and the models described in the previous section, to produce three second level zoning maps. To this purpose, the first step was the application of the consistency model (see Figure 4a) to the results of the two independent analysis, i.e. the statistical and the DInSAR computational maps. Over a total of 1328 TCUs characterized by both analyses, about 60% exhibit consistent information. In particular, 107 units are classified as moving and active ($TCU_{M/A}$); 641 units are classified as not-moving and not-active ($TCU_{NM/NA}$); 278 units are classified as not-moving and active ($TCU_{NM/A}$); 302 units are classified as moving and not-active ($TCU_{M/NA}$). The two confidence models (see Figures 4b-c) were then applied, considering the sample of 748 TCUs reporting consistent information ($TCU_{M/A}$ and $TCU_{NM/NA}$) within the 272 TZUs for which both analyses have been performed.

The implementation of the statistical confidence model produced a statistical state of activity zoning map with confidence level (Figure 11a). The latter shows that high confidence levels may be assigned to: 19 out of 57 TZUs with high activity; 11 out of 47 TZUs with medium activity; 46 out of 69 TZUs with low activity; 54 out of 99 TZUs with very low activity. As a

result, the percentage of TZUs with a high confidence level is higher for the units classified with low and very low activity (60%) than for the ones characterized by medium and high activity (29%). Similarly, the implementation of the DInSAR confidence model produced a DInSAR state of activity zoning map with confidence level (Figure 11b). The map shows that high confidence levels may be assigned to: 29 out of 72 TZUs with high activity; 8 out of 25 TZUs with medium activity; 27 out of 35 TZUs with low activity; 100 out of 140 TZUs with very low activity. In brief, the analyses carried out point out that the confidence level of the TZUs with low and very low activity is much higher than the confidence level of the TZUs with medium and high activity.

The last step of the second level analysis is the application of the combination model (see Figure 4d), which leads to a combined Statistical-DInSAR state of activity zoning map (Figure 11c). To this aim, the two state of activity zoning maps are cross-evaluated to assign, to each TZU which has been characterized by both analyses, one of the following five activity indicators: high activity, medium activity, low activity, very low activity, further scrutiny needed. The latter is used to classify the TZUs for which the original activity indicators differ by more than two levels. Referring to the sample of 272 TZUs, the application of the model highlighted the following classification distribution: 34 high activity TZUs (13%); 42 medium activity TZUs (15%); 53 low activity TZUs (19%); 54 very low activity TZUs (20%); 89 TZUs for which further information is needed (33%).

When only the TZUs characterized by a high confidence level are considered, the application of the combination model yields a final map called “high confidence statistical-DInSAR state of activity zoning map”. As already mentioned during the description of the procedure, this map is based on evaluations showing a very strong level of consistency between the two employed methodologies. Referring to the sample of 169 TZUs classified by both analyses

with high confidence level, the final third level zoning map (Figure 12) is characterized by the following state of activity classification distribution: 31 high activity TZUs (18%); 13 medium activity TZUs (8%); 51 low activity TZUs (30%); 54 very low activity TZUs (32%); 20 TZUs for which further scrutiny is necessary (12%). It is worth noting that by limiting the analysis to the sample of TZUs with high confidence the number of ambiguous cases, for which further information is necessary, reduces from 89 (33% of the TZUs classified within the second level zoning map) to 20 (12% of TZUs classified within the third level zoning map). This is clearly visible also in Figure 13, which reports a chart summarizing the number of TZUs classified by the various zoning maps developed within the three levels of the proposed procedure.

4.2. Validation of the analyses

The obtained results were crosschecked with information deriving from both the ENVISAT sensor dataset—whose acquisition period spans from November 2002 to July 2010—and the analyses carried out over the same area by Cascini et al. (2013a) implementing the so-called "DInSAR-damage matrix".

The first validation check was performed over 143 Terrain Zoning Units, which are units both covered by ENVISAT data and exhibiting a high confidence level according to both the DInSAR (ERS dataset) and the statistical analyses. The subset of the high confidence Statistical-DInSAR (ERS dataset) state of activity zoning map (see Figure 12) covering the considered sample of 143 TZUs shows the following distribution: 23 high activity TZUs; 14 medium activity TZUs; 65 low activity TZUs; 41 very low activity TZUs. The application of the DInSAR activity model (see Figure 3b) using ENVISAT data from 2002 to 2010, over the same sample of TZUs, yields the following distribution: 19 high activity TZUs; 20 medium

activity TZUs; 35 low activity TZUs; 69 very low activity TZUs. The results of the validation check, performed by cross matching the two state of activity distributions, are reported in Table 3 and Figure 14. The results are comforting as they show that during the ENVISAT observation period about 71% of the TZUs (i.e. the number of TZU which are H/M or L/VL according to both ERS and ENVISAT data over the total number of 143 TZU) are confirmed in the state of activity computed, using ERS data, within the high confidence Statistical-DInSAR state of activity zoning map.

The second validation check was performed comparing the high confidence Statistical-DInSAR state of activity zoning map with the results of the implementation of the "DInSAR-damage matrix" (Cascini et al. 2013a) over 91 Terrain Zoning Units. The latter are TZUs covered by the DInSAR-damage matrix and exhibiting a high confidence level according to both DInSAR and statistical analyses. The DInSAR-damage matrix provides the updated state of activity as output in two classes, active (A) and dormant (D), and suggests in situ survey (S) when the available information is not sufficient to assign the new state of activity. The input data to the matrix are the state of activity provided by the landslide inventory map (i.e. active or dormant); the information gathered from the damage survey (i.e. landslide with damage, landslide with no damage, landslide with no damage survey); the condition of movement derived from ERS DInSAR data (i.e. moving or not moving). The results of this validation check are reported in Table 4 and Figure 15. About 60% of the considered TZUs (55 out of 91) do not need in-situ survey or further scrutiny, because they are characterized both according to DInSAR-damage matrix and to the high confidence statistical-DInSAR state of activity zoning map. Considering those, out of the 43 TZUs defined as dormant according to the DInSAR-damage matrix, 33 exhibit very low and low activity according the statistical-DInSAR state of activity zoning map and, out of 12 TZUs assumed as active by the

DInSAR-damage matrix, 4 exhibit high activity in the statistical-DInSAR map. As a result, an overall matching of around 67%, i.e. 37 out of 55 TZUs, is obtained (Table 4). In particular, the types of landslides associated with the matching TZUs are: earth flows (16 out of 20); rotational slides (14 out of 20); rotational slide-earth flow (8 out of 15).

As an example of the potential application of the proposed procedure, Figure 16 shows a landslide, located in the municipal territory of Reino, classified as a dormant earth flow by the landslide inventory. ERS and ENVISAT average velocities over the landslide are respectively equal to 9.8mm/yr and 5mm/yr. The high confidence statistical-DInSAR state of activity zoning map reports, for this landslide, a high level of activity with reference to the period September 1992-December 2000 (see Figure 12). The high level of activity is also confirmed by both: the DInSAR-damage matrix, following a damage survey carried out in 2000 showing cracks on masonry houses located along the boundary of the landslide body (Cascini et al., 2013a); the implementation of the DInSAR activity model using ENVISAT data for the period November 2002 to July 2010. Finally, all the above results were confirmed during an in-situ damage survey carried out in 2012 revealing a wall where the width of the vertical cracks recorded in year 2000 increased as well as the occurrence of some inclined cracks on a wall which previously resulted as crack free (Cascini et al., 2013a).

5. Concluding remarks

Updating landslide inventory maps is an important issue for landslide risk management. Procedures routinely applied to this aim are mainly based on geological/geomorphological analyses, aerial photo-interpretation and in-situ surveys. Yet, when the areas to be zoned are large and an updating frequency of the order of a few years is sought, conventional procedures may turn out to be too expensive and time-consuming. In these cases, the use of

statistical multivariate analyses, on one side, and the exploitation of remote sensing data, on the other side, already proved very valuable in several case studies described in the scientific literature. The paper addressed the issue by proposing an original procedure to classify, via the joint use of statistical multivariate analyses and DInSAR data, existing landforms susceptible to slow landsliding on the basis of their state of activity. The procedure follows a three-level cascade approach which, through cross consistency analyses, assigns a confidence level to state of activity zoning maps derived from both statistical multivariate and DInSAR analyses. The procedure has been successfully applied to a case study in southern Italy. The obtained results were validated via a twofold comparison with: a more recent DInSAR dataset to which the DInSAR activity model was applied; the results of a previous work carried out over the same area which benefited from the information gathered from in situ damage surveys. Both validation tests exhibit matching results around 70%, thus encouraging further applications. As a very important by-product of the analyses, the proposed approach allows the identification of areas requiring further analyses at larger scales. Such assessment may positively influence budget allocation choices performed by Authorities in charge of managing landslide risk over large areas of territory. Indeed, expensive conventional surveys may be planned to be carried out only with reference to those phenomena for which, according to the proposed procedure, further scrutiny is necessary.

The current limits to the use of the described methodology are mostly related to the availability of: reliable inventory of existing landslides and landforms susceptible to landsliding; relevant thematic maps related to landslide predisposing factors, such as geological, geo-hydrological and geomorphological maps; accurate DInSAR data on landslides, often limited by factors related to vegetation cover, satellite orbits, aspect and slope of the terrain. As a result of these limitations, and in particular to the latter one, the

number of landslides whose state of activity can be updated following the proposed procedure may turn out to be rather limited with respect to the total number of mapped landslides. Concerning this, however, it is worth mentioning that the increasing availability and exploitation of very high-resolution SAR data characterized by a relatively short revisiting time—such as those acquired by sensors operating at X-band (i.e. COSMOSkyMed and TERRASAR-X)—will significantly improve the state of the practice, as it will allow an increased and more frequent DInSAR coverage over landslide affected areas.

6. Acknowledgements

The Authors are grateful to the National Basin Authority of Liri-Garigliano and Volturno rivers, and in particular to the general secretary Vera Corbelli, for furnishing all the thematic maps of the study area. The Authors wish also to thank Italian Ministry of the Environment and Protection of Land and Sea, and in particular dr. Salvatore Costabile, for providing the PSI data of the study area deriving from the Piano Straordinario di Telerilevamento Ambientale.

The present work was partially funded by the PRIN project (Programmi di ricerca scientifica di rilevante interesse nazionale) “La mitigazione del rischio da frana mediante interventi sostenibili” supported by Italian Ministry of Education, University and Research, call 2010-2011.

References

Antronico L, Borrelli L, Peduto D, Fornaro G, Gullà G, Paglia L, Zeni G (2013) Conventional and innovative techniques for the monitoring of displacements in landslide affected areas. In: Landslide Science and Practice, Proc. Second World Landslide Forum, Springer-Verlag Berlin 2:125-131

Bai SB, Wang J, Lü GN, Zhou PG, Hou SS, Xu SN (2010) GIS-based logistic regression for landslide susceptibility mapping of the Zhongxian segment in the Three Gorges area, China. Geomorphology 115, 23-31

Baeza C, Corominas J (2001) Assessment of shallow landslide susceptibility by means of multivariate statistical techniques. Earth Surface Processes and Landforms 26:1251-1263

Berardino P, Fornaro G, Lanari R, Sansosti E (2002) A New Algorithm for Surface Deformation Monitoring based on Small Baseline Differential SAR Interferograms. IEEE Transactions on Geoscience and Remote Sensing 40:2375-2383

Bianchini S, Ciampalini A, Raspini F, Bardi F, Di Traglia F, Moretti S, Casagli N (2014) Multi-temporal evaluation of landslide movements and impacts on buildings in San Fratello (Italy) by means of C-band and X-band PSI data. Pure and Applied Geophysics 172:3043-3065

Bonnard Ch, Tacher L, Beniston M (2008) Prediction of landslide movements caused by climate change modelling the behaviour of a mean elevation large slide in the Alps and assessing its uncertainties. In: Landslides and Engineered Slopes – From the past to the future, Proc. 10th International Symposium on Landslides and Engineered Slopes, CRC Press 1:217-227

Calò F, Ardizzone F ,Castaldo R, Lollino P, Tizzani P, Guzzetti F, Lanari R, Angeli MG, Pontoni F, Manunta M (2014) Enhanced landslide investigations through advanced DInSAR techniques The Ivancich case study, Assisi, Italy. Remote Sensing of Environment 1:69-82

Calvello M, Cascini L, Mastroianni S (2013) Landslide zoning over large areas from a sample inventory by means of scale-dependent terrain units. Geomorphology 182:33-48

Carrara A (1983) Multivariate models for landslide hazard evaluation. Mathematical Geology 15(3):403-426

Cascini L, Fornaro G, Peduto D (2009) Analysis at medium scale of low-resolution DInSAR data in slow-moving landslide affected areas. ISPRS J. Photogram. Remote Sens 64:598-611

Cascini L, Fornaro G, Peduto D (2010) Advanced low- and full resolution DInSAR map generation for slow-moving landslide analysis at different scales. Eng Geol 112:29-42

Cascini L, Peduto D, Pisciotta G, Arena L, Ferlisi S, Fornaro G (2013a) The combination of DInSAR and facility damage data for the updating of slow-moving landslide inventory maps at medium scale. Natural Hazards and Earth System Sciences 13:1527-1549

Cascini L, Peduto D, Reale D, Arena L, Ferlisi S, Verde S, Fornaro G (2013b) Detection and monitoring of facilities exposed to subsidence phenomena via past and current generation SARsensors. Journal of Geophysics and Engineering 10:064001

Catani F, Casagli N, Ermini L, Righini G, Menduni G (2005) Landslide hazard and risk mapping at catchment scale in the Arno River basin. Landslides 2:329-342

Chau KT, Chan JE (2005) Regional bias of landslide data in generating susceptibility maps using logistic regression: case of Hong Kong Island. Landslides 2:280-290

Chung CJF, Fabbri AG (1999) Probabilistic prediction models for landslide hazard mapping. Photogrammetric Engineering and Remote Sensing 65:1389-1399

Chung CJF (2006) Using likelihood ratio functions for modeling the conditional probability of occurrence of future landslides for risk assessment. Computers and Geosciences 32:1052-1068

Ciurleo M, Calvello M, Cascini L (2016) Susceptibility zoning of shallow landslides in fine grained soils by statistical methods. Catena 139:250-264

Colesanti C, Wasowski J (2006) Investigating landslides with spaceborne Synthetic Aperture Radar (SAR) interferometry. Eng Geol 88:173-199

Costantini M, Falco S, Malvarosa F, Minati F (2008) A new method for identification and analysis of persistent scatterers in series of SAR images. IEEE Int Geoscience & Remote Sensing Symposium, II:449-452

Crosetto M, Biescas E, Duro J (2008) Generation of advanced ERS and Envisat interferometric SAR products using the stable point network technique. Photogram. Eng. Remote Sens., 4:443-450

Cruden DM, Varnes DJ (1996) Landslides Types and Processes. In: Landslides Investigation and Mitigation, National Academy of Sciences Special Report 247:36–75

Dai FC, Lee CF (2002) Landslide characteristics and slope instability modelling using GIS, Lantau Island, Hong Kong. Geomorphology 42:213-228

D'Elia B, Rossi-Doria M (2000) Slow movements of earthflow accumulations along the Ionic Coast (South-Eastern Italy). In: Landslides in research, theory and practice, Proc 8th Int Symp Landslides, Thomas Telford London 1:439–446

Dewitte O, Chung C, Cornet Y, Daoudi M, Demoulin A (2010) Combining spatial data in landslide reactivation susceptibility mapping a likelihood ratio-based approach in W Belgium. Geomorphology 122:153-166

Ermini L, Catani F, Casagli N (2005) Artificial neural networks applied to landslide susceptibility assessment. Geomorphology 66:327-343

Fell R, Ho KKS, Lacasse S, Leroi E (2005) A framework for landslide risk assessment and management. In: Landslide Risk Management, Taylor & Francis London 3-25

Fell R, Corominas J, Bonnard C, Cascini L, Leroi E, Savage WZ (2008) Guidelines for landslide susceptibility, hazard and risk zoning for land use planning. Eng Geol 102:85-98

Ferlisi S, Peduto D, Gullà G, Nicodemo G, Borrelli L, Fornaro G (2015) The use of DInSAR data for the analysis of building damage induced by slow-moving landslides. In: Engineering Geology for Society and Territory, Springer Switzerland 2:1835-1839

Ferretti A, Prati C, Rocca F (2000) Nonlinear Subsidence Rate Estimation Using Permanent Scatterers in Differential SAR Interferometry. IEEE Transactions on Geoscience and Remote Sensing 38:2202-2212

Ferretti A, Prati C, Rocca F (2001) Permanent scatterers in SAR interferometry. IEEE Transactions on Geoscience and Remote Sensing 39:8-20

Fornaro G, Reale D, Serafino F (2009) Four-dimensional SAR imaging for height estimation and monitoring of single and double scatterers. IEEE Transactions on Geoscience and Remote Sensing 47:224-237

Fumagalli A, Novali F, Prati C, Rocca F, Rucci A (2011) A New Algorithm for Processing Interferometric Data-StacksSqueeSAR. IEEE Transactions on Geoscience and Remote Sensing 49:3460-3470

Gullà G, Peduto D, Borrelli L, Antronico L, Fornaro G (2016) Geometric and kinematic characterization of landslides affecting urban areas: the Lungro case study (Calabria, Southern Italy). Landslides, DOI 10.1007/s10346-015-0676-0, article in press

Guzzetti F, Carrara A, Cardinali M, Reichenbach P (1999) Landslide hazard evaluation a review of current techniques and their application in a multi-scale study, Central Italy. Geomorphology 31:181-216

Guzzetti F, Reichenbach P, Cardinali M, Galli M, Ardizzone F (2005) Probabilistic landslide hazard assessment at the basin scale. Geomorphology 72:272-299

Herrera G, Notti D, Garcia-Davalillo JC, Mora O, Cooksley G, Sanchez M, Arnaud A, Crosetto M (2011) Analysis with C- and X-band satellite SAR data of the Portalet landslide area. Landslides 8:195-206

Lee S, Ryu JH, Kim IS (2007) Landslide susceptibility analysis and its verification using likelihood ratio, logistic regression, and artificial neural network models case study of Youngin, Korea. Landslides 4:327-338

Lu P, Catani F, Tofani V, Casagli N (2014) Quantitative hazard and risk assessment for slow-moving landslides from Persistent Scatterer Interferometry. Landslides 11:685-696

Mansour MF,Morgenstern NR, Martin CD (2011) Expected damage from displacement of slow-moving slides. Landslides 7:117-131

Mathew J, Jha VK, Rawat GS (2007) Weights of evidence modelling for landslide hazard zonation mapping in part of Bhagirathi valley, Uttarakhand. Current Science 92:628-638

Meisina C, Zucca F, Notti D, Colombo A, Cucchi A, Savio G, Giannico C, Bianchi M (2008) Geological Interpretation of PSInSAR Data at Regional Scale. Sensors 8:7469-7492

Nefeslioglu HA, Gokceoglu C, Sonmez H (2008) An assessment on the use of logistic regression and artificial neural networks with different sampling strategies for thepreparation of landslide susceptibility maps. Engineering Geology 97:171-191

Notti D, Davalillo JC, Herrera G, Mora O (2010) Assessment of the performance of X-band satellite radar data for landslide mapping and monitoring Upper Tena Valley case study. Nat.Hazards Earth Syst. Sci. 10:1865-1875

Peduto D, Arena L, Calvello M, Anzalone R, Cascini L (2015a) Evaluating the state of activity of slow-moving landslides by means of DInSAR data and statistical analyses. In: Proc XVI ECSMGE Geotechnical Engineering for Infrastructure and Development, ICE Publishing 4:1843-1848

Peduto D, Cascini L, Arena L, Ferlisi S, Fornaro G, Reale D (2015b) A general framework and related procedures for multiscale analyses of DInSAR data in subsiding urban areas. ISPRS Journal of Photogrammetry and Remote Sensing 105:186-210

Peduto D, Pisciotta G, Nicodemo G, Arena L, Ferlisi S, Gullà G, Borrelli L, Fornaro G, Reale D (2016) A procedure for the analysis of building vulnerability to slow-moving landslides. In: Proc 1st IMEKO Int Work Metrology for Geotechnics, Athena Srl Benevento 248-254

Picarelli L, Russo C (2004) Remarks on the mechanics of slow active landslides and the interaction with man-made works. In: Landslides – Evaluation & Stabilization, Proc 9th Int Sym Landslides, Balkema 2:1141-1176

Pourghasemi HR, Pradhan B, Gokceoglu C(2012) Application of fuzzy logic and analytical hierarchy process (AHP) to landslide susceptibility mapping at Haraz watershed, Iran. Natural Hazards 63:965-996,

Pradhan B, Ohb HJ, Buchroithner M (2010) Weights-of-evidence model applied to landslide susceptibilty mapping in a tropical hilly area. Geomatics Natural Hazards and Risk 1:199-223

Rapolla A, Di Nocera S, Matano F, Paoletti V, Tarallo D (2012) Le aree dei terreni complessi del Sannio e dell'Irpinia. In: Criteri di zonazione della suscettibilità e della pericolosità da frane innescate da eventi estremi (piogge e sisma), Composervice Srl Padova 238–248 (in Italian)

Rossi M, Guzzetti F, Reichenbach P, Mondini AC, Peruccacci S (2010) Optimal landslide susceptibility zonation based on multiple forecasts. Geomorphology 114:129-142

Spizzichino D, Falconi L, Delmonaco G, Margottini C, Puglisi C (2004) Integrated approach for landslide risk assessment of Crago Village (Italy). In: Landslides – Evaluation & Stabilization, Proc 9th Int Sym Landslides, Balkema 1:237-242

Taskin K, Emrehan KS, Ismail C (2015) An assessment of multivariate and bivariate approaches in landslide susceptibility mapping a case study of Duzkoy district. Natural Hazards 76:471-496

Thiery Y, Malet JP, Sterlacchini S, Puissant A, Maquaire O (2007) Landslide susceptibility assessment by bivariate methods at large scales application to a complex mountainous environment. Geomorphology 92:38-59

Tofani V, Segoni S, Agostini A, Catani F, Casagli N (2013) Use of remote sensing for landslide studies in Europe. Nat. Hazards Earth Syst. Sci. 13:299-309

Urciuoli G, Picarelli L (2008) Interaction between landslides and man-made works. In: Landslides and Engineered Slopes – From the past to the future. Proc 10th Int Sym Landslides and Engineered Slopes, CRC Press 2:1301-1307

Van Den Eeckhaut M, Vanwalleghem T, Poesen J, Govers G, Verstraeten G, Vandekerckhove L (2006) Prediction of landslide susceptibility using rare events logisticregression: a case-study in the Flemish Ardennes (Belgium). Geomorphology 76:392-410

Van Westen CJ (2004) Geo-information tools for landslide risk assessment: an overview of recent developments. In: Landslides Evaluation and Stabilization. Proc. 9th Int Sym Landslides, Balkema 1:39-56

Varnes DJ (1978) Slope Movement Types and Processes. In: Landslides Analysis and Control, National Research Council Special Report 176:11-33

Varnes DJ (1984) Landslide hazard zonation: a review of principles and practice. UNESCO Paris

Wang FW, Wang G, Zhang YM, Huo ZT, Peng XM, Araiba K, Takeuchi A (2008) Displacement Monitoring on Shuping Landslide in the Three Gorges Dam Reservoir Area, China from August 2004 to July 2007. In: Landslides and Engineered Slopes – From the past to the future. Proc 10th Int Sym Landslides and Engineered Slopes, CRC Press 2:1321-1327

Wasowski J, Bovenga F (2014) Investigating landslides and unstable slopes with satellite Multi Temporal Interferometry: Current issues and future perspectives. Engineering geology 174:103-138

Wei M, Sandwell DT (2010) Decorrelation of L-band and C-band interferometry over vegetated areas in California, IEEE Transactions on Geoscience and Remote Sensing 48:2942-2952

Yin KJ, Yan TZ (1988) Statistical prediction model for slope instability of metamorphosed rocks. Proc 5th Int Sym Landslides, Taylor & Francis 2:1269-1272

Zhang L, Liao M, Balz T, Shi X, Jiang Y (2014) Monitoring landslide activities in the three gorges area with multi-frequency satellite SAR data sets. In: Modern technologies for landslide investigation and prediction, Springer Berlin 181-208

List of Acronyms

DInSAR = Differential SAR Interferometry

H = High activity

hc = High confidence

IA_D = DInSAR Index of Activity

IA_S = Statistical Index of Activity

$IC_{M/A}$ = True-positives Consistency Index

$IC_{NM/NA}$ = True-negatives Consistency Index

L = Low activity

lc = Low confidence

M = Medium activity

TCU = Terrain Computational Unit

TCU_a = Active Terrain Computational Unit

TCU_c = Terrain Computational Unit covered by DINSAR data

TCU_{cm} = Terrain Computational Unit covered by DINSAR data and moving

$TCU_{M/A}$ = Terrain Computational Unit moving according to the DInSAR analysis and active according to the statistical analysis

$TCU_{M/NA}$ = Terrain Computational Unit moving according to the DInSAR analysis and not active according to the statistical analysis

$TCU_{NM/A}$ = Terrain Computational Unit not moving according to the DInSAR analysis and active according to the statistical analysis

$TCU_{NM/NA}$ = Terrain Computational Unit not moving according to the DInSAR analysis and not active according to the statistical analysis

TCU_{tot} = Total number of Terrain Computational Units

TZU = Terrain Zoning Unit

VL = Very Low activity

Table 1. Classification in 8 classes, using a quantile criterion, of the six numerical variables employed in the statistical analysis.

Class	V1 (m)	V2 (°)	V3 (m^{-1})	V4 (m)	V5 (m)	V6 (m)
1	48 to 188	0 to 3	-71.00 to -15.01	0 to 55	0 to 93	0 to 340
2	189 to 302	4 to 7	-15.00 to -2.01	56 to 117	94 to 210	341 to 581
3	303 to 397	8 to 10	-2.00 to -0.81	118 to 188	211 to 349	582 to 827
4	398 to 489	11 to 14	-0.80 to -0.19	189 to 269	350 to 519	828 to 1097
5	490 to 592	15 to 19	-0.18 to 0.32	270 to 367	520 to 740	1098 to 1406
6	593 to 705	20 to 27	0.33 - 1.25	368 to 491	741 to 1042	1407 to 1778
7	706 to 825	28 to 46	1.26- 9.71	492 to 658	1043 to 1482	1779 to 2268
8	826 to 1107	47 to 83	9.72 - 46.77	659 to 1081	1483 to 2464	2269 to 3461

Table 2. Comparison of the state of activity of the TZUs classified by: the statistical analysis, considering both the full sample of 1372 TZUs and the sample of 272 TZUs also characterized by the DInSAR analysis; the DInSAR analysis.

State of activity from…	High	Medium	Low	Very Low
Statistical analysis (1372 TZUs characterized)	374 (27%)	210 (15%)	205 (15%)	583 (42%)
Statistical analysis (272 TZUs characterized)	57 (21%)	47 (17%)	69 (25%)	99 (36%)
DInSAR analysis (272 TZUs characterized)	72 (26%)	25 (9%)	35 (13%)	140 (51%)

Table 3. Validation check performed by cross matching the high confidence Statistical-DInSAR state of activity zoning map [ERS dataset] with the results of the DInSAR activity model [ENVISAT dataset] over 143 Terrain Zoning Units.

		From "DInSAR activity model" [ENVISAT dataset]			
		H (19 TZUs)	M (20 TZUs)	L (35 TZUs)	VL (69 TZUs)
From "high confidence statistical-DInSAR state of activity zoning map" [ERS dataset]	H (23 TZUs)	6	5	3	9
	M (14 TZUs)	3	3	5	3
	L (65 TZUs)	6	10	20	29
	VL (41 TZUs)	4	2	7	28

Table 4. Validation check performed by cross matching the high confidence Statistical-DInSAR state of activity zoning map [ERS dataset] with the results of the DInSAR-damage matrix (Cascini et al. 2013) over 91 Terrain Zoning Units.

		From "DInSAR damage matrix" [ERS dataset]		
		A (13 TZUs)	D (47 TZUs)	S (31 TZUs)
From "high confidence statistical-DInSAR state of activity zoning map" [ERS dataset]	H (12 TZUs)	4	6	2
	M (6 TZUs)	0	4	2
	L (38 TZUs)	4	18	16
	VL (25 TZUs)	4	15	6
	S (10 TZUs)	1	4	5

List of Figures

Figure 01 Click here to download Figure Figure01.pptx

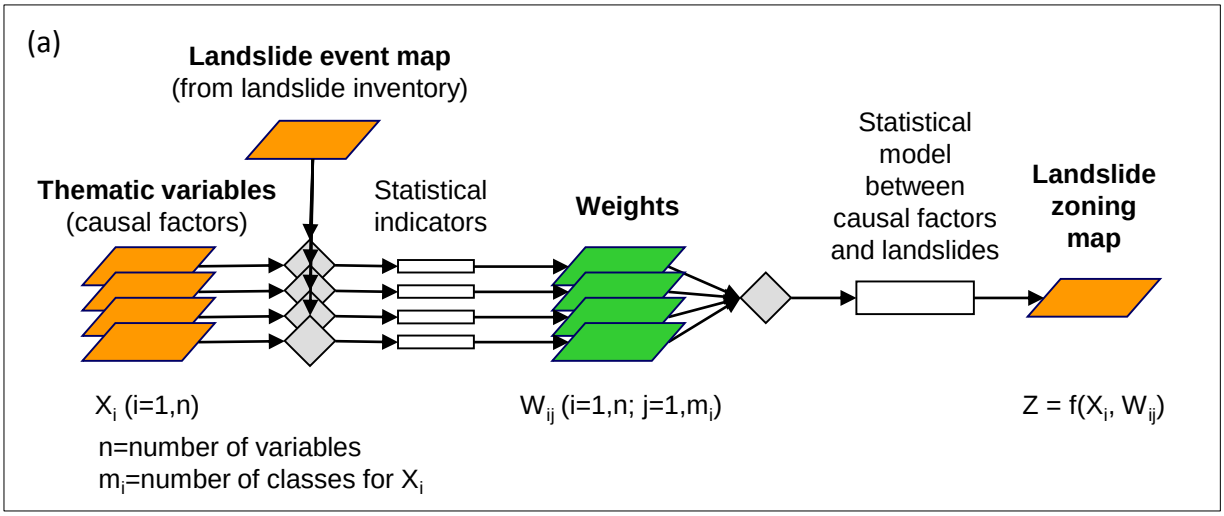

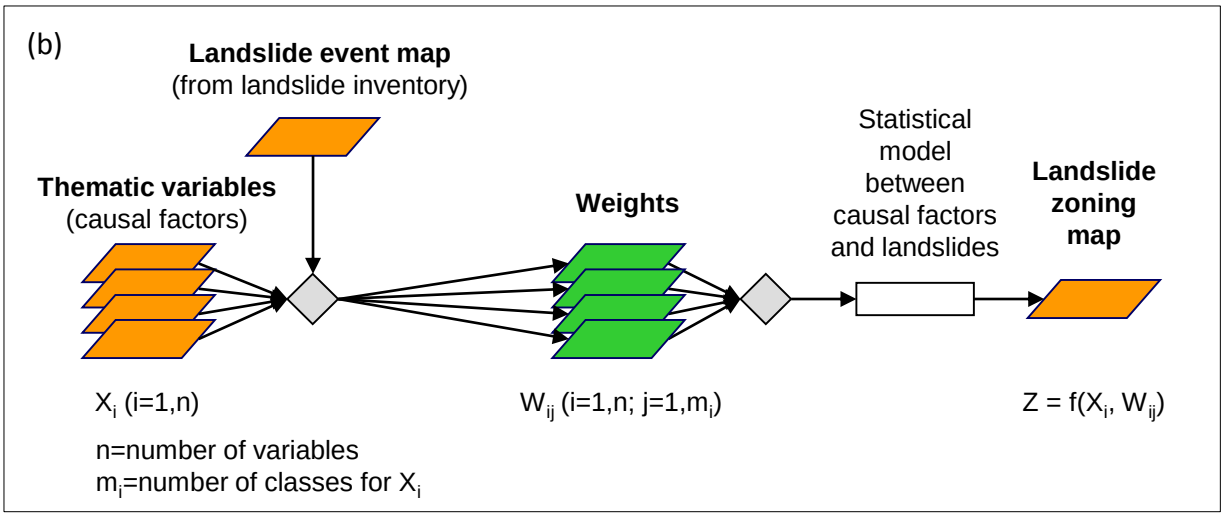

Figure 02

Click here to download Figure Figure02_NEW.pptx

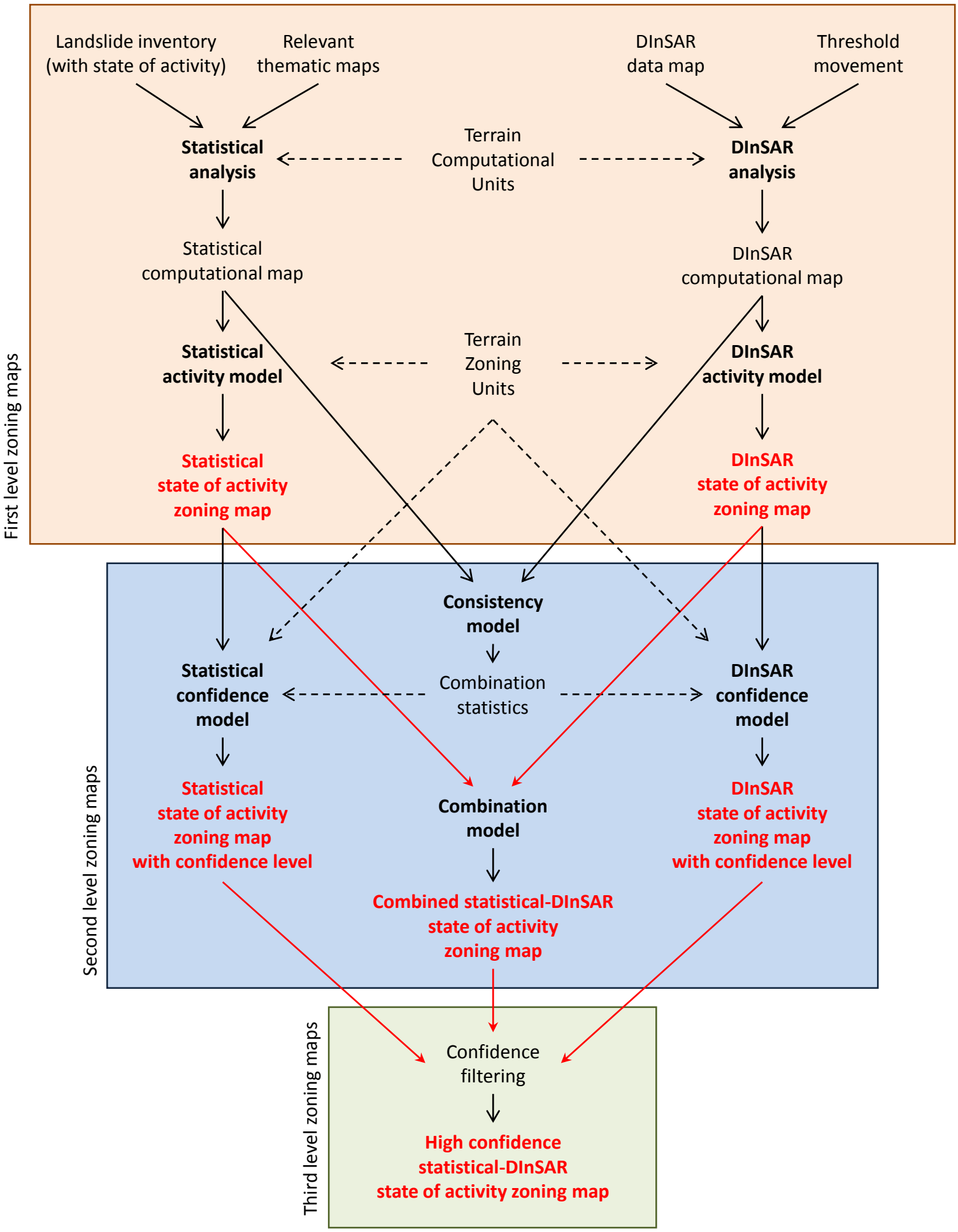

Figure 03

Statistical activity model

Statistical Index of Activity		
	$0.70 \leq IA_S \leq 1.00$	H
	$0.35 \leq IA_S < 0.70$	M
	$0.05 \leq IA_S < 0.35$	L
	$IA_S \leq 0.05$	VL

(a)

DInSAR activity model

DInSAR Index of Activity		
	$0.70 \leq IA_D \leq 1.00$	H
	$0.35 \leq IA_D < 0.70$	M
	$0.05 \leq IA_D < 0.35$	L
	$IA_D \leq 0.05$	VL

(b)

Figure 04

(a) Consistency model

		DInSAR computational map: Moving	DInSAR computational map: Not Moving
Statistical computational map	Active	$TCU_{M/A}$	$TCU_{NM/A}$
	Not Active	$TCU_{M/NA}$	$TCU_{NM/NA}$

(b) Statistical confidence model

		$IC_{M/A}$ <50%	$IC_{M/A}$ >50%	$IC_{NM/NA}$ <50%	$IC_{NM/NA}$ >50%
Statistical state of activity zoning map	High	S_H_{lc}	S_H_{hc}		
	Medium	S_M_{lc}	S_M_{hc}		
	Low			S_L_{lc}	S_L_{hc}
	Very Low			S_VL_{lc}	S_VL_{hc}

(c) DInSAR confidence model

		$IC_{M/A}$ <50%	$IC_{M/A}$ >50%	$IC_{NM/NA}$ <50%	$IC_{NM/NA}$ >50%
DInSAR state of activity zoning map	High	D_H_{lc}	D_H_{hc}		
	Medium	D_M_{lc}	D_M_{hc}		
	Low			D_L_{lc}	D_L_{hc}
	Very Low			D_VL_{lc}	D_VL_{hc}

(d) Combination model

		DInSAR state of activity zoning map: H	M	L	VL
Statistical state of activity zoning map	H	H	H	M	S
	M	H	M	M	S
	L	M	M	L	L
	VL	S	S	L	VL

Figure 05

Click here to download Figure Figure05.pptx

Combination model with confidence filtering		DInSAR state of activity zoning map with confidence level			
		D_H_{hc}	D_M_{hc}	D_L_{hc}	D_VL_{hc}
Statistical state of activity zoning map with confidence level	S_H_{hc}	H_{hc}	H_{hc}	M_{hc}	S
	S_M_{hc}	H_{hc}	M_{hc}	M_{hc}	S
	S_L_{hc}	M_{hc}	M_{hc}	L_{hc}	L_{hc}
	S_VL_{hc}	S	S	L_{hc}	VL_{hc}

Figure 06

Click here to download Figure Figure06_NEW.pptx

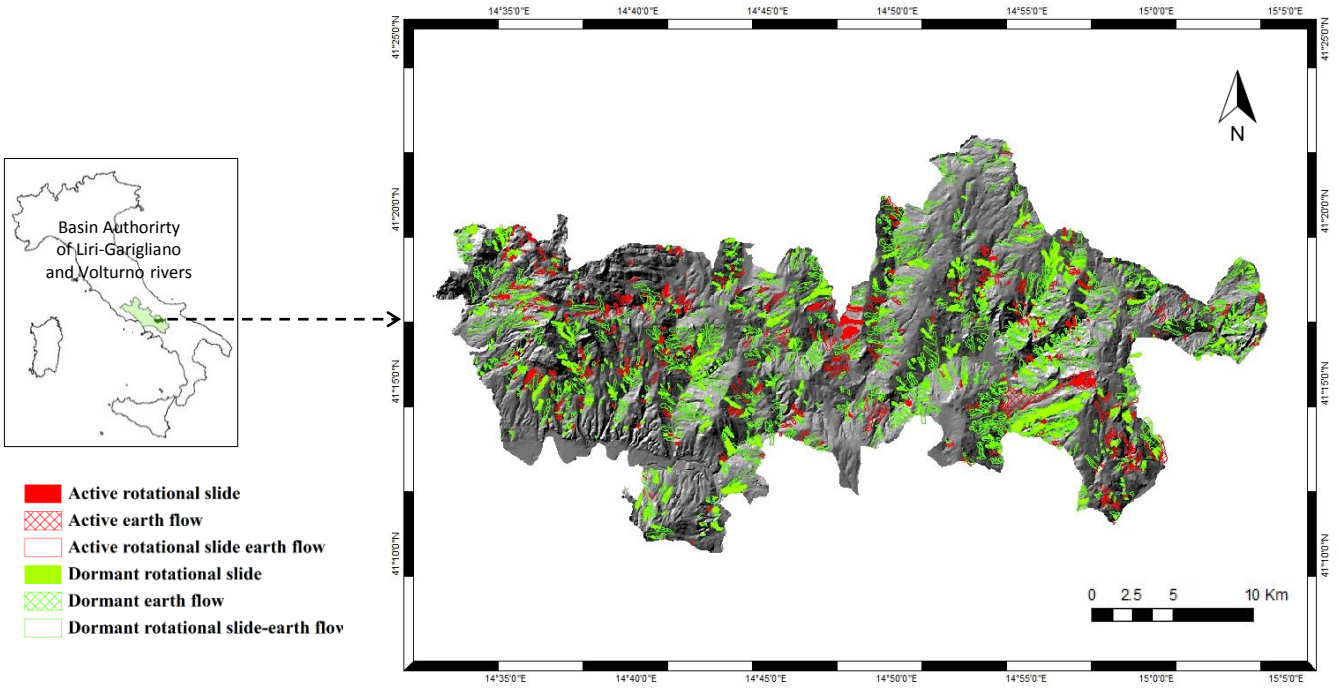

Figure 07

Click here to download Figure Figure07.pptx

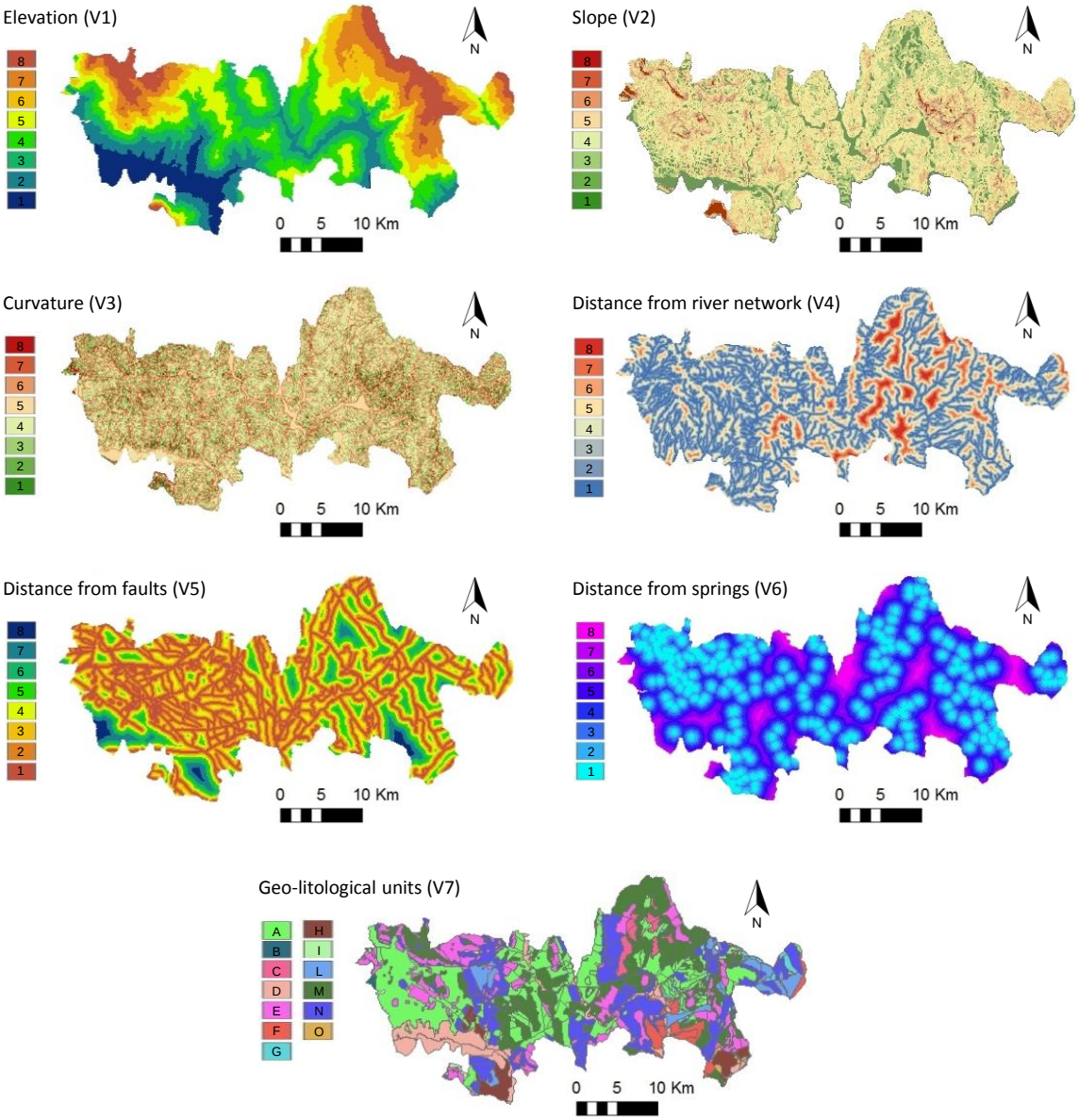

Figure 08

Click here to download Figure Figure08.pptx

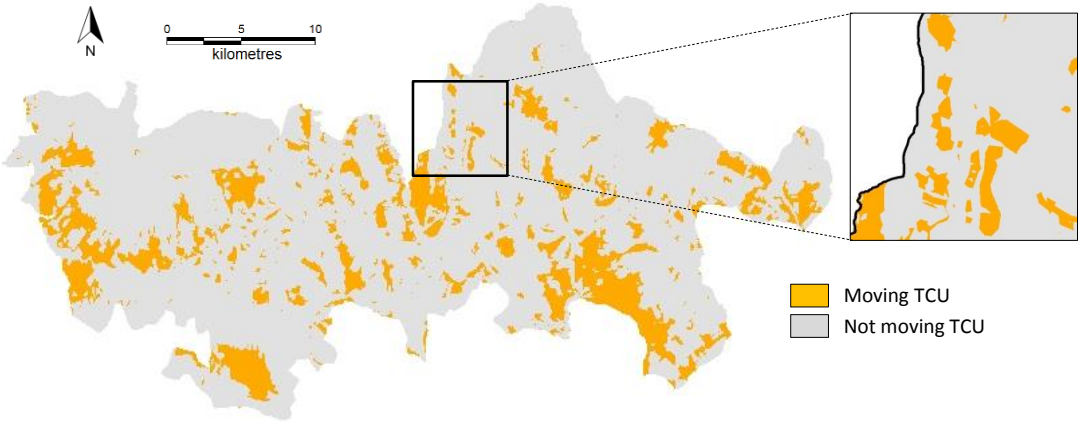

(a)

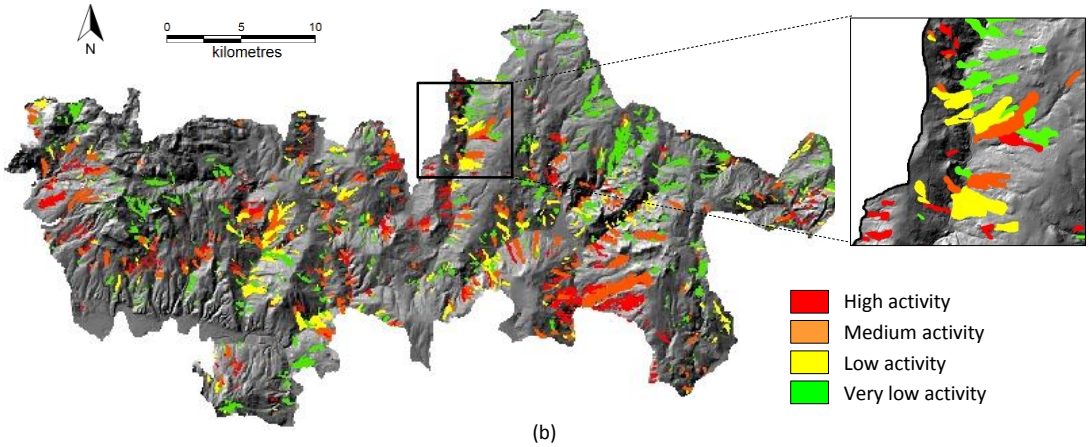

(b)

Figure 09

Click here to download Figure Figure09.pptx

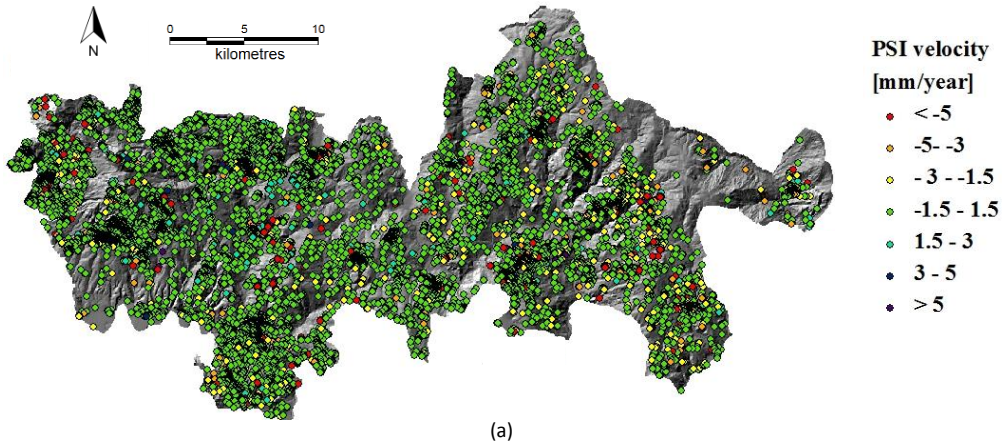

(a)

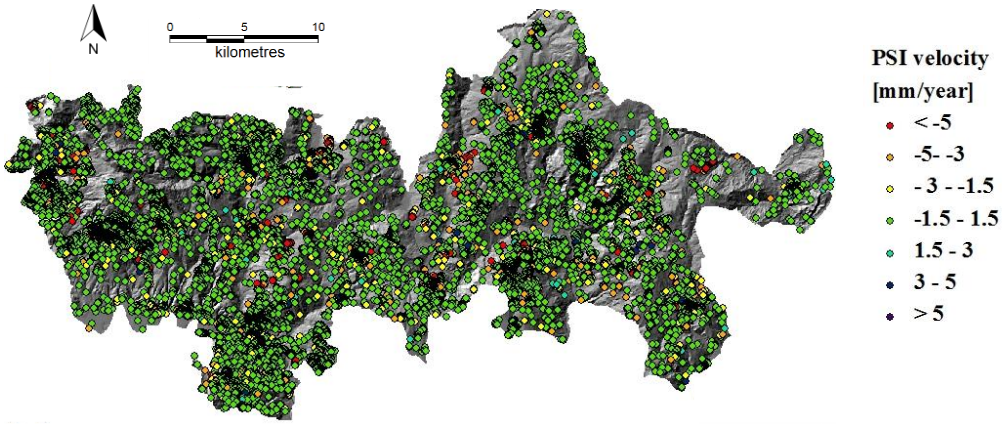

(b)

Figure 10

Click here to download Figure Figure10.pptx

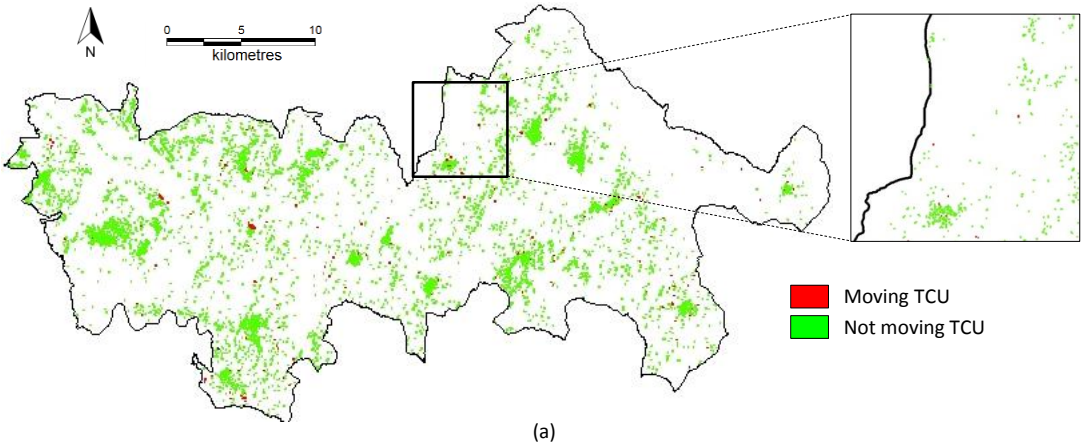

(a)

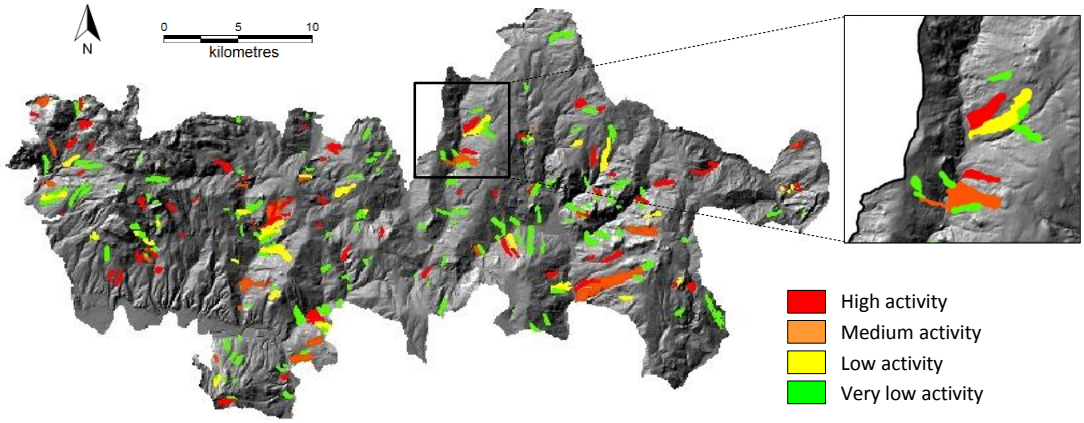

(b)

Figure 11

Click here to download Figure Figure11.pptx

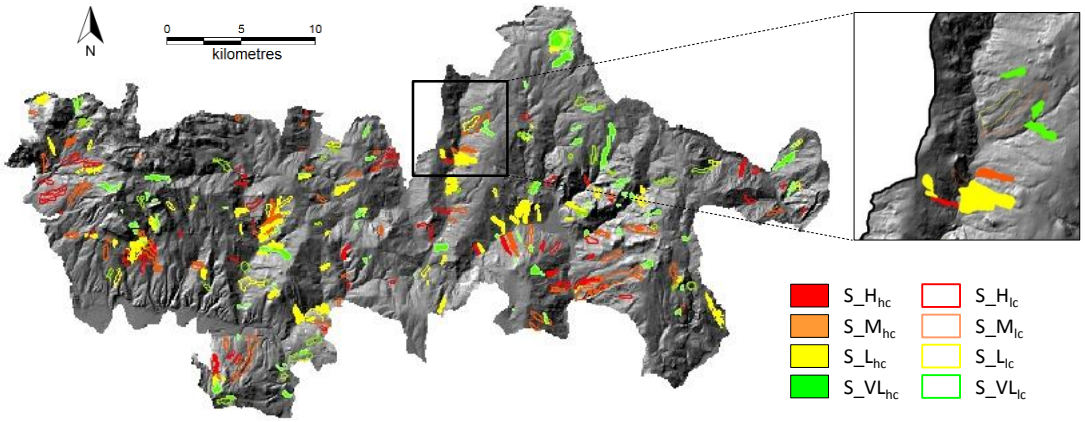

(a)

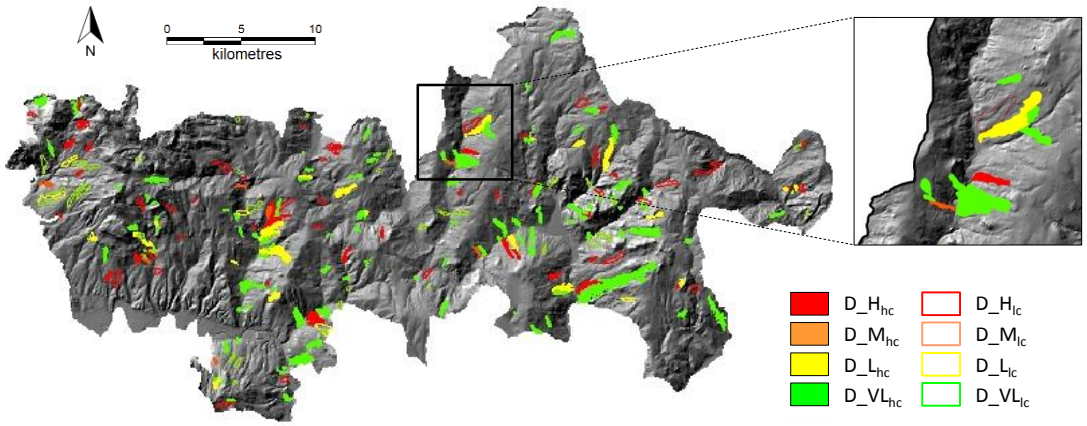

(b)

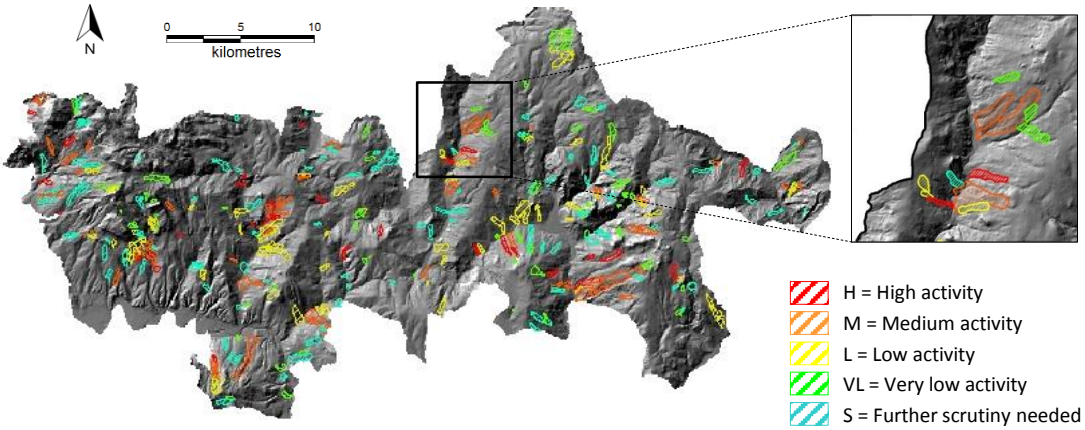

(c)

Figure 12

Click here to download Figure Figure12.pptx

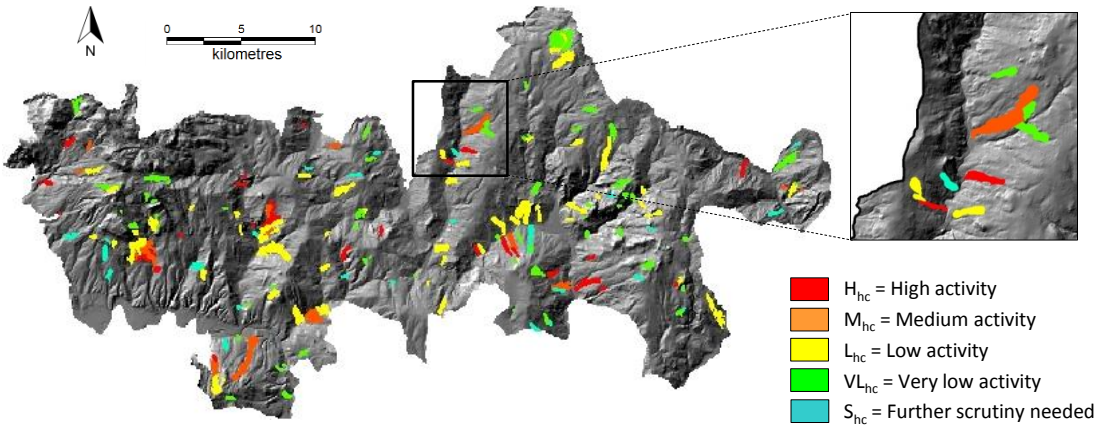

Figure 13

Click here to download Figure Figure13.pptx

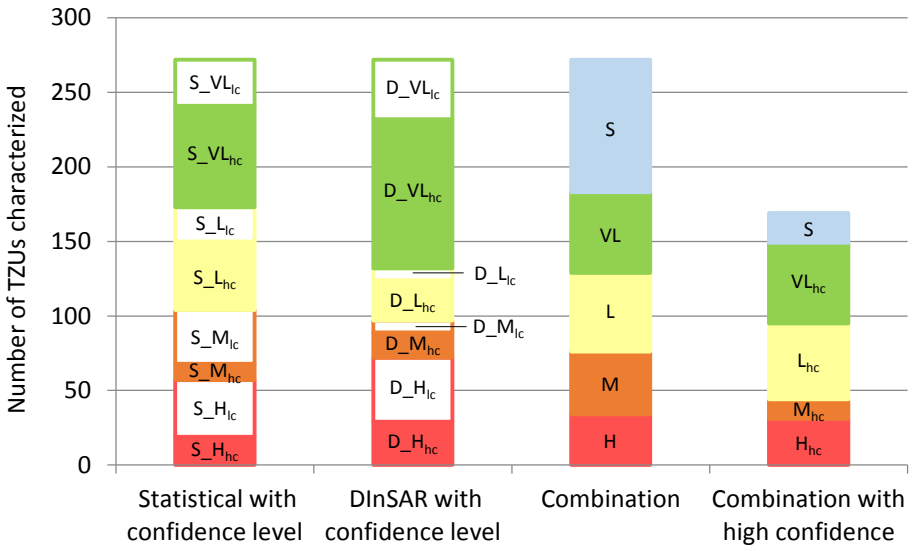

Figure 14

Click here to download Figure Figure14_NEW.pptx

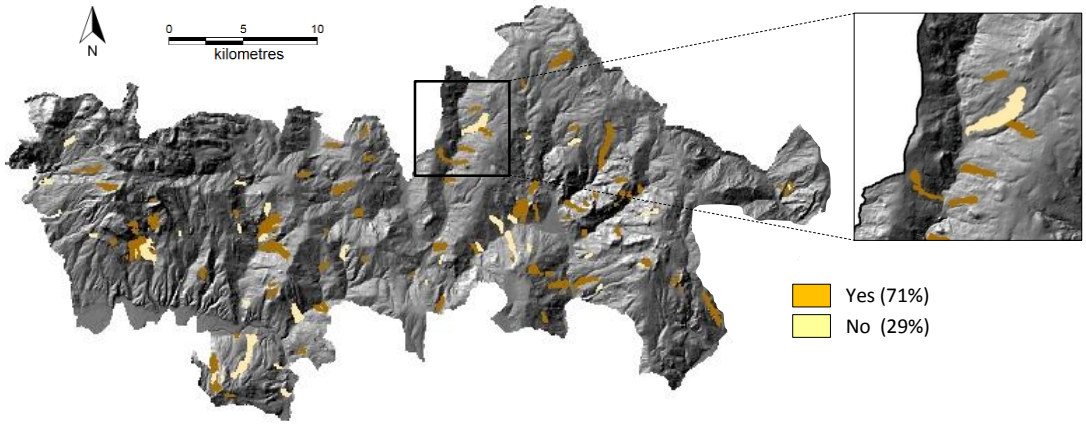

Figure 15

Click here to download Figure Figure15_NEW.pptx

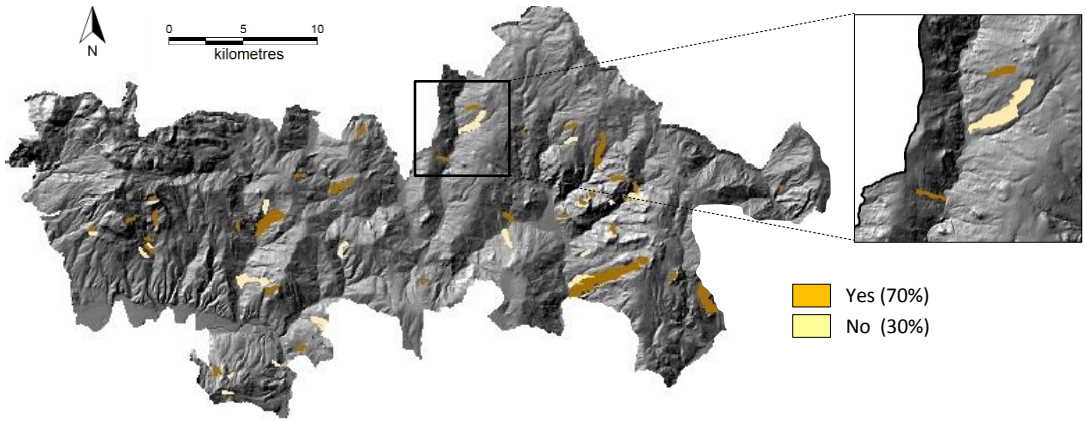

Figure 16

Click here to download Figure Figure16.pptx